Compatibility of alkaline earth metal (Mg, Ca, Sr)-doped lanthanum chromites as separators in planar-type high-temperature solid oxide fuel cells

M. MORI, T. YAMAMOTO, H. ITOH, T. WATANABE
Chemical Energy Engineering Department, Chemical Power Generation Group, Central Research Institute of Electric Power Industry, 2-6-1 Nagasaka, Yokosuka, Kanagawa 240-01, Japan

The mechanical, electrical and thermal properties of alkaline earth metal (Mg, Ca and Sr)-doped $LaCrO_3$ have been examined as separators in planar-type high-temperature solid oxide fuel cells. The maximum three-point bending strength at 1000 °C in air was measured and found to be 186 MPa for $LaCr_{0.9}Mg_{0.1}O_3$, 36 MPa for $La_{0.9}Ca_{0.1}CrO_3$ and 77 MPa for $La_{0.9}Sr_{0.1}CrO_3$. The $La_{0.8}Sr_{0.2}CrO_3$ separator placed in both an oxidizing and a reducing environment at 1000 °C showed almost the same electrical conductivities of the H_2 atmosphere, and the conductivity was independent of sample thickness in the range 0.5–3.0 mm. For all the doped $LaCrO_3$ perovskites, a difference between the thermal expansion behaviours of air and the H_2 atmosphere was observed. In particular, the thermal expansion slope for the first heating cycle under the H_2 atmosphere showed a marked change. The volume changes were due to the formation of oxygen defects in the perovskite structure.

1. Introduction

In recent years, there has been a growing interest in the realization of high-temperature solid oxide fuel cell (SOFC) systems capable of byproduct high-quality heat. A SOFC system with a high efficiency could be applied to a wide variety of constructible electric power generation systems ranging from small co-generation systems to large power plants. Of all cell configurations, the planar cell design is high in power density per volume (watts per cubic centimetre), short in electric conductivity paths and low in production cost. However, many technological challenges for developing materials are still necessary to obtain a planer-type SOFC with a high performance.

Alkaline earth metal (AE = Mg, Ca or Sr)-doped lanthanum chromites are considered to be very promising materials for use as a separator or interconnector in a SOFC. The reason for this is that AE-doped lanthanum chromites have excellent chemical stability under oxidizing or reducing atmospheres at operating temperatures of around 1000 °C [1]. In addition, they have high electronic conductivities and show compatibility in thermal expansion properties with the other cell components in an oxidizing atmosphere [2–4]. However, in low oxygen partial pressures (less than 10^{-4} atm) at operating temperatures of 1000 °C or above, AE-doped lanthanum chromites, La(Cr, Mg)$O_{3-\delta}$ and (La, Ca, Sr)$CrO_{3-\delta}$, show oxygen deficiency, δ, in the perovskite structures. The deficiency increases with decreasing oxygen partial pressure, P_{O_2}, and results in lower electrical conductivity and larger thermal expansion than those in high P_{O_2} according to the δ value [5]. Under the reducing atmosphere, a drastic decrease in the electrical conductivity has been observed [4, 7, 8], and some fundamental data for the thermal properties have also been reported [1]. In fact, the separators when placed in a SOFC are exposed to both oxidizing and reducing environments at the operating temperature. Therefore, the electrical conductivity and thermal expansion behaviours of AE-doped lanthanum chromites in an oxygen potential gradient are quite important.

For the planar-type SOFC, a serious problem is the generation of thermal stress in the stack since this cell configuration tends to produce a large temperature difference in the plane direction under the operating condition at around 1000 °C. To decrease the temperature difference, an excellent thermal conductivity is desired to the separator. Furthermore, in the case of a separator self-supported planar-type SOFC stack, where the separator provides the mechanical strength to the stack, the mechanical strength to the separator, especially at the operating temperature, is quite important.

In this study, we have investigated the mechanical strengths, electrical conductivities and thermal

0022–2461

properties in air and a H_2 atmosphere for the AE-doped lanthanum chromites with different dopants and discussed application as a separator in the planar-type SOFC.

2. Experimental procedure

The AE-doped $LaCrO_3$ powders were synthesized using the ordinary ceramic powder preparation method. The starting material powders, La_2O_3 (pre-heated at 1500 °C for 1 h), $SrCO_3$, $CaCO_3$, MgO (pre-heated at 1200 °C for 4 h) and Cr_2O_3 powders were obtained from Nakarai, Japan, and used without further purification. The powders in the desired proportions were thoroughly mixed with acetone in a rotary-type Y_2O_3-partially-stabilized ZrO_2 ball mill for 24 h. After being dried, the mixtures were rapidly heated to 1400 °C in air for 1 h and held at this temperature for 8 h. The milling and heating procedures were repeated twice. To obtain the dense tablets with relative densities over 95%, the powders were mixed with an ethanol solution of paraffin and pressed into a tablet under a pressure of 98 MPa. Then, the tablets were calcined at 800 °C in a N_2 stream to dehydrate and were eventually sintered at 1900 °C for 1 h in a carbon furnace under flowing argon gas (greater than 99.999%), i.e., an Ar–CO atmosphere. Table I shows the full chemical compositions measured by inductively coupled plasma (ICP) analysis. The chemical compositions of the prepared lanthanum chromites were almost identical with those of the starting materials, and the amounts of impurities of Al and Si were less than 0.012 mol %. All the samples were confirmed by X-ray diffraction (XRD) analysis (JEOL JDX-8030).

The bending strength measurement was performed in a three-point bending apparatus at room temperature, 500 °C and 1000 °C. The dimensions of specimens with relative densities over 95% were 36 mm × 4 mm × 3 mm. The span length was 20 mm and the ramp speed was 3.0 mm min^{-1}. For measurements at high temperatures, the sample was heated in air at a rate of 5.0 °C min^{-1} and held for 10 min before measuring.

The direct current (d.c.) four-terminal method using Pt wires was used to measure the electrical conductivity in air and a H_2 atmosphere in the temperature range from 500 to 1000 °C. The measurement was carried out after the conductivity in air 1000 °C showed no change with time. On the other hand, the electrical conductivity of $La_{0.8}Sr_{0.2}CrO_3$, which was placed in both air and a H_2 atmosphere, was measured at 1000 °C by a d.c. four-terminal method as shown in Fig. 1. Pt meshes with four Pt terminals were attached to the $La_{0.8}Sr_{0.2}CrO_3$ tablet using Pt paste and firing at 1000 °C for 1 h. The cell was tightened by springs to decrease the contact electrical resistance. It was made gas tight using Pyrex glass. A flow rate of 100 ml min^{-1} of air or H_2 gas was used during these measurements.

The thermal diffusivity was measured by a laser flush method using Shinkuriko TC-7000 equipment. The specific heat was measured by thermal differential scanning calorimetry using Ulvac HPC-7000 equipment. These measurements were performed at room temperature using tablets (about 2 mm thick and 12 mm in diameter). The thermal conductivity was calculated from the following equation

$$\lambda = \alpha \rho C_p \quad (1)$$

where λ is the thermal conductivity, α is the thermal diffusivity, ρ is the density and C_p is the specific heat. The value λ was corrected by the following Maxwell–Eucken equation

$$\lambda_0 = \lambda \frac{(1 + 0.5p)}{(1 - p)} \quad (2)$$

TABLE I Chemical composition (mol %) of the AE-doped lanthanum chromites

Sample	La	Mg	Ca	Sr	Cr
$LaCrO_3$	100	—	—	—	100.4
$LaCr_{0.9}Mg_{0.1}O_3$	100	9.4	—	—	93.5
$LaCr_{0.8}Mg_{0.2}O_3$	100	18.7	—	—	18.1
$La_{0.9}Ca_{0.1}CrO_3$	91.3	—	9.7	—	100
$La_{0.8}Ca_{0.2}CrO_3$	79.5	—	18.6	—	100
$La_{0.7}Ca_{0.3}CrO_3$	70.0	—	28.5	—	100
$La_{0.9}Sr_{0.1}CrO_3$	91.1	—	—	9.8	100
$La_{0.8}Sr_{0.2}CrO_3$	79.4	—	—	19.7	100
$La_{0.7}Sr_{0.3}CrO_3$	70.4	—	—	30.0	100

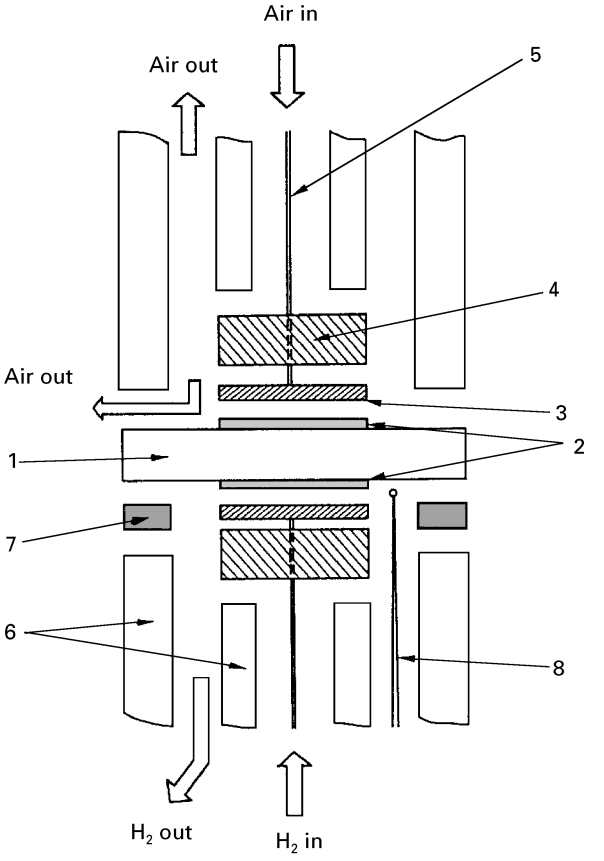

Figure 1 Experimental equipment for electrical conductivity measurement of the $La_{0.8}Sr_{0.2}CrO_3$ placed in a SOFC atmosphere. 1, lanthanum chromite tablet; 2. Pt electrode; 3, Pt mesh; 4, honeycomb-like cordierite; 5, Pt wire; 6, alumina tube; 7, Pyrex 0-ring packing; 8, thermocouple.

where λ_0 is the thermal conductivity of the polycrystal with a relative density of 100%, and p is the porosity.

Thermogravimetry–differential thermal analysis measurements were carried out using Mac Science TG-DTA 2020S equipment in the temperature range from room temperature to 1000 °C. The average linear thermal expansion coefficient (TEC) was measured using a Mac Science TD-5000S system with an Al_2O_3 reference in the temperature range from 50 to 1000 °C. A heating rate of 5 °C min^{-1} and a flow rate of 100 ml min^{-1} of air or H_2 gas were used in these measurements after those gases had been bubbled through pure water at 10 °C.

3. Results and discussion

3.1. Mechanical strength

Fig. 2 shows the three-point bending strength of the 10 mol % AE-doped lanthanum chromites at room temperature, 500 °C and 1000 °C. The error bars represent the standard deviations from five independent measurements. The maximum bending strengths of the perovskites at the selected temperatures are summarized in Table II. There was a significant difference between the mechanical strengths of the doped lanthanum chromites with different dopants; the maximum strengths at room temperature were 418 MPa, 166 MPa and 269 MPa for $LaCr_{0.9}Mg_{0.1}O_3$, $La_{0.9}Ca_{0.1}CrO_3$ and $La_{0.9}Sr_{0.1}CrO_3$, respectively. Since the mechanical strength of ceramics, in general, decreases with increasing temperature, the strength of the chromites drastically decreases with increasing temperature, too. In particular, $La_{0.9}Ca_{0.1}CrO_3$ showed the poorest bending strength of 36 MPa at 1000 °C. Quite recently, Sammes *et al.* [9] have also reported a similar temperature dependence of the mechanical strengths for $La_{1-x}Sr_xCrO_3$ ($x = 0.1$–0.3) samples at temperatures between 600 and 1000 °C, and the strength increased with increasing Sr content.

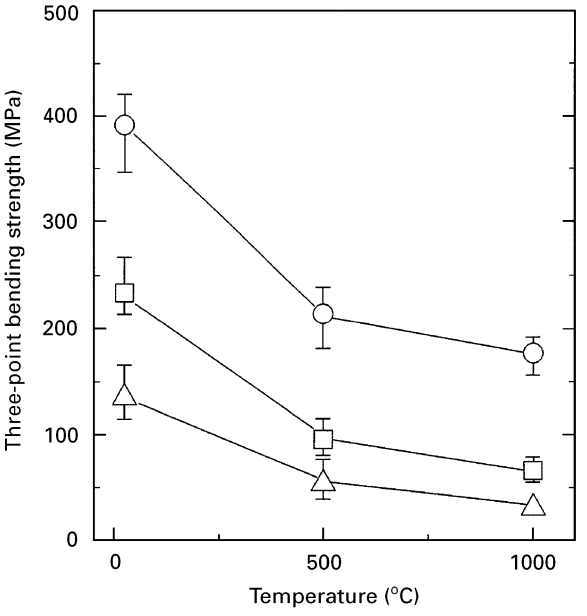

Figure 2 3-point bending strength of the AE-doped lanthanum chromite as a function of temperature. (○), $LaCr_{0.9}Mg_{0.1}O_3$; (△), $La_{0.9}Ca_{0.1}CrO_3$; (□), $La_{0.9}Sr_{0.1}CrO_3$.

Sintering mechanisms such as solid-state sintering, liquid-phase sintering and reaction sintering affect the microstructures of sintered ceramics, and the mechanical strength is strongly dependent on the microstructure. For the 10 mol % AE-doped $LaCrO_3$, it has been reported that the sintering mechanisms under a low-P_{O_2} atmosphere were solid-state sintering for Mg-doped $LaCrO_3$ and liquid-phase sintering for Ca- or Sr-doped $LaCrO_3$ [10]. The $LaCr_{0.9}Mg_{0.1}O_3$ specimens consisted of a small grain size of 3–6 μm through solid-state sintering, whereas the grain growth of $La_{0.9}Ca_{0.1}CrO_3$ and $La_{0.9}Sr_{0.1}CrO_3$ specimens through liquid-phase sintering was more marked than that of the Mg-doped specimens. As shown in Fig. 2, the difference between the mechanical strengths of the Ca- and Sr-doped chromites might be caused by the different melting points of the liquid phases, i.e., the different contents of liquid phases [10]. Thus, these results on the sintering mechanisms were in good agreement with those on the strength measurements, and the lowering of the strength for the A-site substitutions corresponded to the decrease in the surface energy of the particle due to grain growth. The relationship between the sintering mechanism and the strength suggests that, to develop new AE-doped $LaCrO_3$ separators with a high mechanical strength, grain growth by liquid-phase sintering during the sintering process should be prevented as little as possible. Note that it is well known that the air-sinterable lanthanum calcium chromites with a B-site deficit, namely $(La, Ca)_{1+y}CrO_3$, have a liquid-phase sintering mechanism [11, 12]. The results of three-point bending strength measurement on $La_{0.9}Ca_{0.12}CrO_3$, which was sintered in air at 1600 °C for 5 h, were very similar to those on $La_{0.9}Ca_{0.1}CrO_3$.

3.2 Electrical conductivity

Pure $LaCrO_3$ is a p-type conductor and shows a low electrical conductive value of approximately

TABLE II Maximum bending strengths of the AE-doped lanthanum chromites

Temperature (°C)	Maximum bending strength (MPa)			
	$LaCr_{0.9}Mg_{0.1}O_3$	$La_{0.9}Ca_{0.1}CrO_3$	$La_{0.9}Sr_{0.1}CrO_3$	$La_{0.9}Ca_{0.12}CrO_3$
Room temperature	418	166	269	150
500 °C	243	77	106	106
1000 °C	186	36	77	33
Sintering mechanism	Solid	Liquid	Liquid	Liquid

0.6–1.0 S cm^{-1} at 1000 °C in air [7]. It can be occupied by Mg^{2+} ions (0.086 Å) with a small ionic radius substituted for Cr^{3+} ions (0.0755 Å) at the B site, and by Ca^{2+} ions (0.114 Å) and Sr^{2+} ions (0.132 Å) with a large ionic radius at the A site. AE doping results in charge compensation by oxidizing Cr^{3+} to Cr^{4+} ions in an oxidizing atmosphere below 1400 °C [5], and the electrical conductivity becomes higher by two orders of magnitude than that of pure $LaCrO_3$. The conduction mechanism of AE-doped lanthanum chromites in air is the exchange reaction of an electron between Cr^{3+} and Cr^{4+} ions. The conductivity should be due to thermally activated hopping of small polarons [13]. The electrical conductivity of AE-doped lanthanum chromites can be expressed by the following equation:

$$\sigma = \frac{1}{T}\frac{e^2a^2}{6k_B\tau_0}[Cr^{3+}][Cr^{4+}]\exp\left(-\frac{E}{k_BT}\right) \qquad (3)$$

where σ is the electrical conductivity, T is the absolute temperature, e is the elementary electric charge, a is the distance of jump, k_B is the Boltzmann factor, τ_0 is the average free time, $[Cr^{3+}]$ and $[Cr^{4+}]$ are the mole fractions and E is the activation energy for conduction.

Fig. 3. shows the temperature dependences of electrical conductivity in air or the H_2 atmosphere for AE-doped lanthanum chromites with different dopant contents. The electrical conductivity in air is well represented by Equation 3. B-site-substituted lanthanum magnesium chromites showed a lower conduction than A-site-substituted samples because of the decrease in Cr ion concentration. For the A-site substitution, the conductivity increased with increasing dopant content. The Ca-doped lanthanum chromites

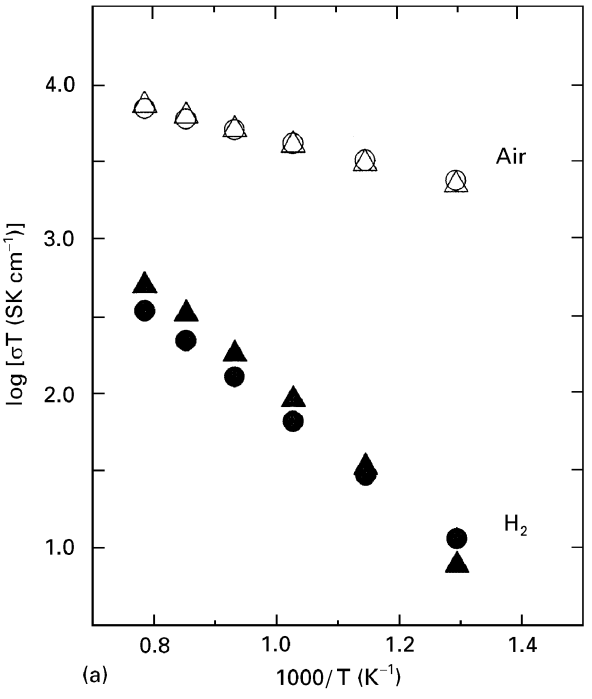

Figure 3 Temperature dependence of electrical conductivity in air or the H_2 atmosphere for the AE-doped lanthanum chromites: (a) $LaCr_{1-x}Mg_xO_3$;(b) $La_{1-x}Ca_xCrO_3$; (c) $La_{1-x}Sr_xCrO_3$. (○), (●), $x = 0.1$; (△), (▲), $x = 0.2$; (□), (■), $x = 0.3$.

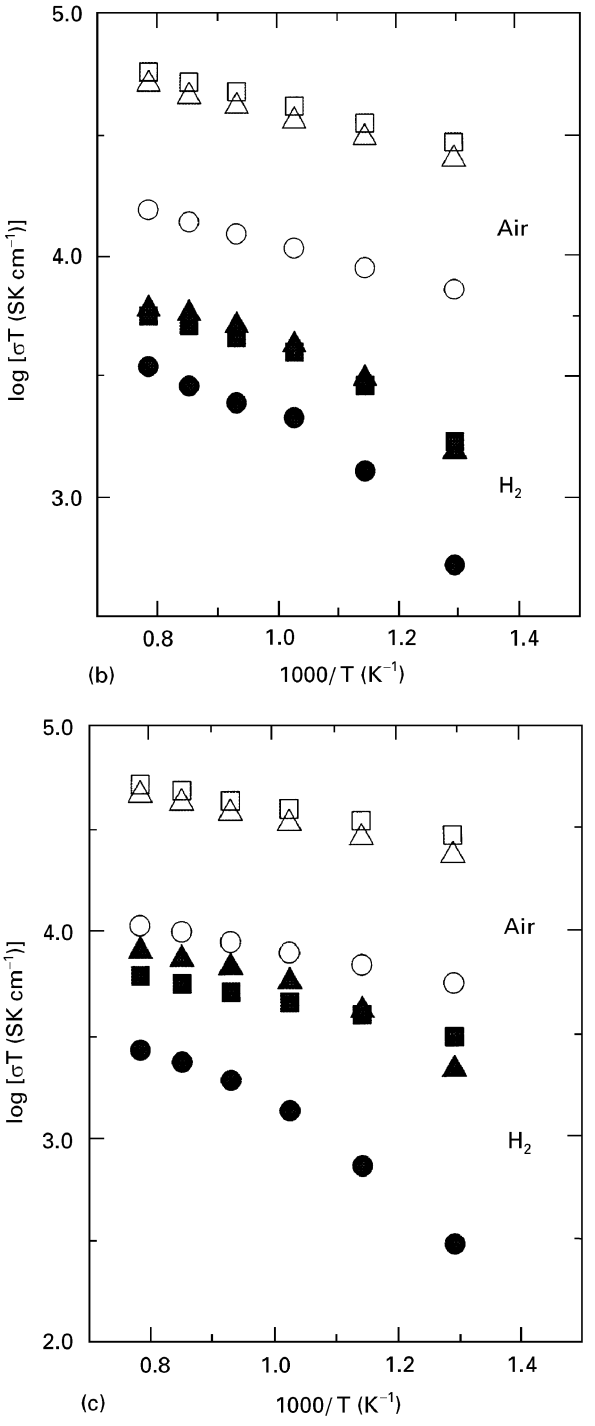

Figure 3 (Continued)

have higher electrical conductivities than the Sr-doped samples do; however, the difference was not drastic. The difference might be explained by the difference in the hopping of electrons from Cr^{3+} to Cr^{4+} ions, because the lattice parameters of the Ca-doped perovskites were smaller than those of the Sr-doped perovskites. Under a reducing atmosphere, a charge compensation of Cr^{4+} to Cr^{3+} ions occurs by the formation of oxygen defects [5]. The electrical conductivities of the doped $LaCrO_3$ in the H_2 atmosphere did not show a linear temperature dependence, because the concentration of oxygen defects depends on P_{O_2} and temperature. Mg-doped $LaCrO_3$ has the lowest conductivity in the H_2 atmosphere. For the A-site substitution case, the electrical conductivities

of $La_{1-x}Ca_xCrO_3$ is lower than those of $La_{1-x}Sr_xCrO_3$ under a reducing atmosphere although the reverse was observed in air. The reason for the difference in the conduction can be explained by the difference in oxygen defect concentration between Ca-doped and Sr-doped lanthanum chromites [14, 15]. The electrical conductivities of all the doped lanthanum chromites at 1000 °C in various atmospheres are summarized in Table III.

Many researchers have reported that $LaMO_3$ (M = transition metals)-based perovskite structure have a non-stoichiometry of the O site and high chemical diffusion coefficient of oxide ions [13, 14]. An oxide-ionic leak current has been proposed for the doped $LaCrO_3$ separator in an oxygen potential gradient [15–17]. The phenomenon of the leak current is quite an important factor not only in lowering the efficiency of the SOFC system but also in determining the oxygen potential profile of the separator placed in both an oxidizing and a reducing environments, because the condition of the oxygen potential profile affects significantly the electrical conductivity of the SOFC separator.

Fig. 4 shows the electrical conductivity of $La_{0.8}Sr_{0.2}CrO_3$ in the oxygen potential gradient between air and the H_2 atmosphere at 1000 °C as a function of sample thickness. After supplying the H_2 gas, a drastic decrease in electrical conductivity was observed with time, and the oxygen defect diffusion coefficient calculated from these measurements was about $(3–4) \times 10^{-6}$ cm^2 s^{-1}. The broken line represents the measured electrical conductivity using a rectangular sample in a H_2 atmosphere, and the lower conductive values are those of the tablet samples in comparison with those of the rectangular sample. The reason for this small difference might be due to contact resistance. During the stationary state, oxygen permeation takes place in series at the surface, and the reaction consists of oxygen reduction and formation of holes. These holes and their association are quite important, because there is a possibility that the surface reaction rate may affect the magnitude of the permeation rate of oxygen. Quite recently, it has also been reported that, for the doped lanthanum chromites, oxide ion diffusion at the grain boundary was faster than in the bulk, especially near the side of higher P_{O_2}. This phenomenon results in a more complicated determination of the oxygen potential profile in the $LaCrO_3$ separator [18, 19]. Even so, in this study, it was found that the electrical conductivity of $La_{0.8}Sr_{0.2}CrO_3$ exposed in both the oxidizing and the reducing atmospheres was essentially governed by that in the reducing atmosphere, because the process of the surface reaction at the side of higher P_{O_2} might be the slowest and rate limiting in the reaction for oxygen permeation [20]. Furthermore, the electrical conductivity of $La_{0.8}Sr_{0.2}CrO_3$ placed in both the SOFC atmospheres was independent of the sample thickness, and the result indicates that the oxygen potential profiles in the $La_{0.8}Sr_{0.2}CrO_3$ separator is independent of the sample thickness in this range. The low electrical characteristic limits the power density when this material is used in separator applications.

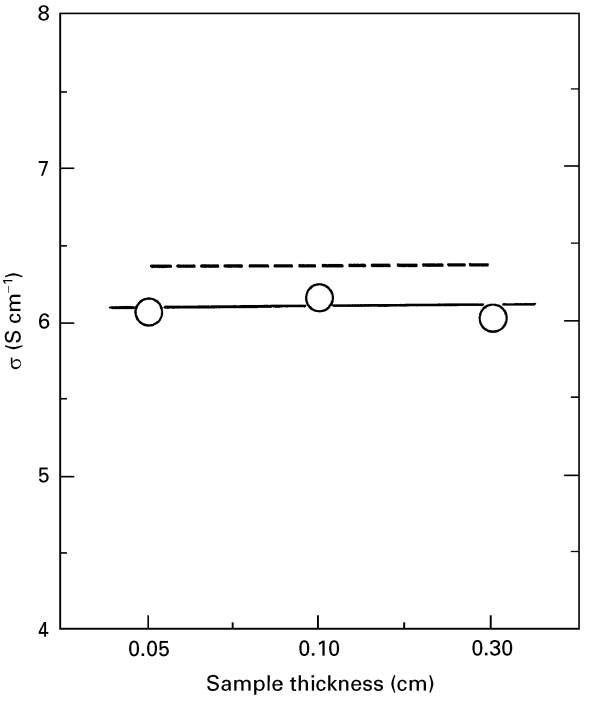

Figure 4 Electrical conductivity of $La_{0.8}Sr_{0.2}CrO_3$ placed in the oxygen potential gradient between air and hydrogen at 1000 °C as a function of sample thickness. (– – –) Rectangular sample.

TABLE III Electrical conductivities of the AE-doped lanthanum chromites at 1000 °C in various atmospheres

Sample	Electrical conductivity (S cm^{-1})		
	In air	In Ar	In H_2
$LaCr_{0.9}Mg_{0.1}O_3$	5.6	5.6	0.27
$LaCr_{0.8}Mg_{0.2}O_3$	5.9	5.6	0.39
$La_{0.9}Ca_{0.1}CrO_3$	12.1	12.1	2.7
$La_{0.8}Ca_{0.2}CrO_3$	40.0	38.7	4.8
$La_{0.7}Ca_{0.3}CrO_3$	45.7	45.5	4.4
$La_{0.9}Sr_{0.1}CrO_3$	8.5	8.3	2.1
$La_{0.8}Sr_{0.2}CrO_3$	36.6	26.6	6.4
$La_{0.7}Sr_{0.3}CrO_3$	41.5	40.4	4.9

3.3. Thermal properties

To calculate thermal stress in the stack under the operating condition, thermal conductivities of AE-doped lanthanum chromites are one of the most important factors. Sakai *et al.* [21] have reported the thermal conductivities for non-doped and Ca-doped $LaCrO_3$: the conductivity of $LaCrO_3$ was about 3.8 W m^{-1} K^{-1} and decreased with increasing temperature. In the Ca-doped $LaCrO_3$ case, the conductivity of $La_{0.9}Ca_{0.1}CrO_3$ was around 2 W m^{-1} K^{-1} at room temperature and decreased with increasing Ca content because of increasing phonon scattering as a thermal conductive carrier. However, no temperature dependence was observed in the calcium-doped dopant. The thermal conductivities of 10 mol % AE-doped $LaCrO_3$ at room temperature are summarized in Table IV. $LaCr_{0.9}Mg_{0.1}O_3$ showed the highest thermal conductivity of 3.1 W m^{-1} K^{-1}. The reason

TABLE IV Thermal properties of the AE-doped lanthanum chromites at room temperature

Sample	Thermal diffusivity	Specific heat	Thermal conductivity ($W m^{-1} K^{-1}$)	
	α ($cm^2 s^{-1}$)	C_p ($J g^{-1} K^{-1}$)	λ	λ_0
$LaCr_{0.9}Mg_{0.1}O_3$	0.0110	0.44	3.1	3.3
$La_{0.9}Ca_{0.1}CrO_3$	0.0083	0.44	2.4	2.5
$La_{0.9}Sr_{0.1}CrO_3$	0.0082	0.44	2.3	2.5

for this is that anharmonicity of lattice vibration increases with increasing atomic weight difference between the elements in the perovskite structure and this causes phonon scattering. Also, the scattering makes the mean free path short and the thermal conductivity low. For the case of A-site substitution, $La_{0.9}Ca_{0.1}CrO_3$ has a thermal conductivity value of 2.5 $W m^{-1} K^{-1}$ comparable with that of $La_{0.9}Sr_{0.1}CrO_3$.

Since the planar-type SOFC incorporates various ceramic composite plates consisting of anode, electrolyte, cathode and separator, it is necessary to match their thermal expansion behaviours. The TEC of yttria-fully-stabilized zirconia (YSZ) electrolyte is approximately $10 \times 10^{-6} °C^{-1}$ in the temperature range from room temperature to the operating temperature of 1000 °C. From the viewpoint of thermal expansion among SOFC components, since the TEC of YSZ is constant regardless of P_{O_2} and composition, the other cell components should have the same TECs. This can be achieved by controlling their compositions. Fig. 5 shows the thermal expansion behaviour of the AE-doped $LaCrO_3$ from room temperature to 1000 °C in air. The TECs increased with increasing AE-dopant content. However, the lattice parameters of the doped $LaCrO_3$ perovskites at room temperature decreased with increasing AE content. This is due to the increase in concentration of Cr^{4+} (0.069 Å) with smaller ionic radius in comparison with that of Cr^{3+} (0.0755 Å) at the octahedral site. This discrepancy will disappear if the thermal expansions of the divalent AE ions are assumed to be larger than that of the trivalent ion. As shown in Fig. 5, there are anomalies for the thermal expansion slopes of the doped lanthanum chromites with the low AE contents, and the temperatures are near 250 °C for the undoped $LaCrO_3$, 330 °C for the Mg-doped chromites and 350 °C for $La_{0.9}Ca_{0.1}CrO_3$. The anomalies are due to a phase transformation from orthorhombic to rhombohedral symmetry with a volume change [22, 23]. In the case of the $La_{0.9}Sr_{0.1}CrO_3$ perovskite, a phase transformation from orthorhombic to rhombohedral symmetry was observed near 80 °C. [24]. In air, the thermal expansion behaviours of all the perovskites during the second heating cycle were very similar to those during the first heating cycle, because no oxygen deficiencies and excesses were observed in this range of temperature.

Fig. 6a and b show the linear thermal expansions of the AE-doped lanthanum chromites in the H_2 atmosphere during the first and second cycles, respectively. For measurements made in the H_2 atmosphere, no

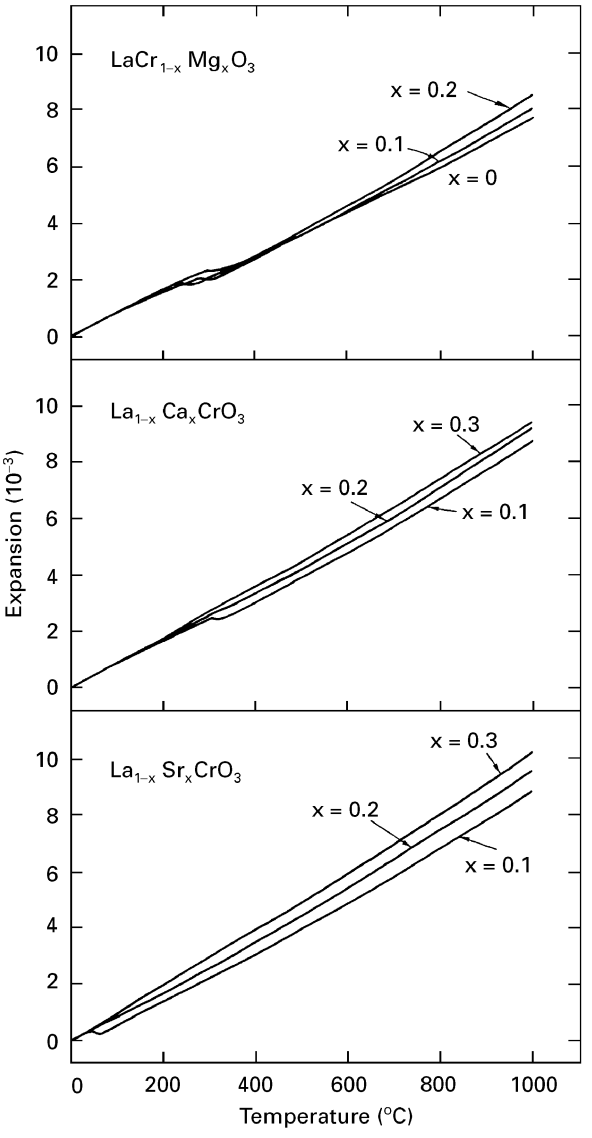

Figure 5 Linear thermal expansion of the AE-doped lanthanum chromites from room temperature to 1000 °C in air.

difference between the results for the second and third heating cycles was observed. However, the doped lanthanum chromites with high AE content showed remarkable anomalies for the thermal expansion behaviours during the first heating cycle, and the degrees of the change depended on the amount of La substitution by Ca or Sr and the amount of Cr substitution by Mg. The temperatures of the first anomalies for their thermal expansion slopes are summarized in Table V. The average linear TECs of the doped $LaCrO_3$ in the temperature range from 50 to 1000 °C are listed in

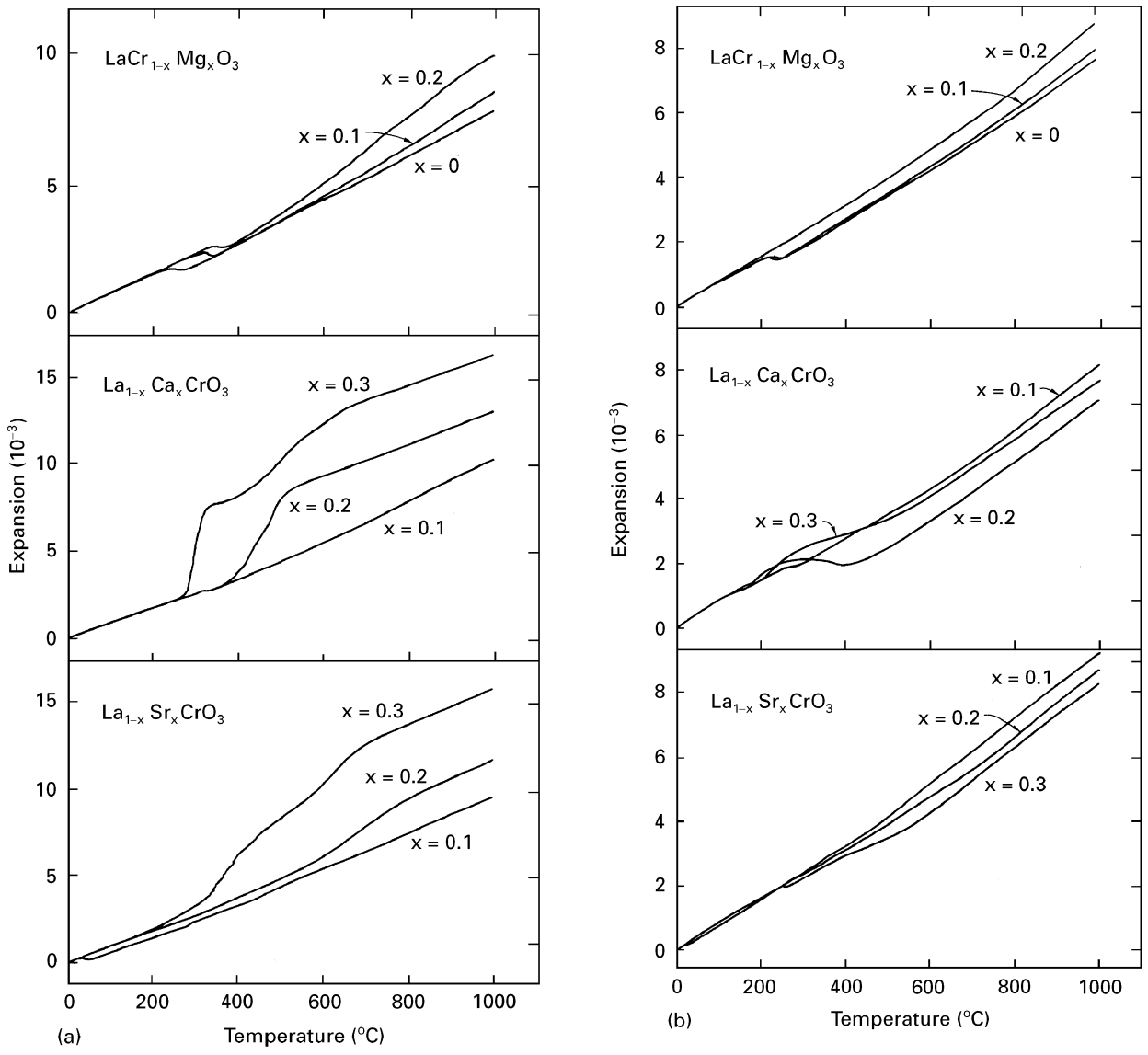

Figure 6 Linear thermal expansion of the AE-doped lanthanum chromites in the H_2 atmosphere: (a) first cycle; (b) second cycle.

TABLE V First anomalous temperatures for thermal expansion slopes of the AE-doped lanthanum chromites in air or the H_2 atmosphere

Sample	First anomalous temperature (°C)		
	In air	In H_2	
	First cycle	First cycle	Second cycle
$LaCrO_3$	246	253	277
$LaCr_{0.9}Mg_{0.1}O_3$	326	334	264
$LaCr_{0.8}Mg_{0.2}O_3$	345	350	—
$La_{0.9}Ca_{0.1}CrO_3$	303	299	313
$La_{0.8}Ca_{0.2}CrO_3$	—	403	284
$La_{0.7}Ca_{0.3}CrO_3$	—	292	—
$La_{0.9}Sr_{0.1}CrO_3$	68	51	55
$La_{0.8}Sr_{0.2}CrO_3$	—	327	208
$La_{0.7}Sr_{0.3}CrO_3$	—	338	—

TABLE VI Average linear TECs of the AE-doped lanthanum chromites in air or the H_2 from 50 to 1000 °C

Sample	TEC (10^6 °C^{-1})		
	In air	In H_2	
	First cycle	First cycle	Second cycle
8YSZ	10.0	9.9	9.9
$LaCrO_3$	8.0	8.1	8.2
$LaCr_{0.9}Mg_{0.1}O_3$	8.4	9.0	8.4
$LaCr_{0.8}Mg_{0.2}O_3$	8.9	10.4	9.1
$La_{0.9}Ca_{0.1}CrO_3$	9.0	9.7	8.5
$La_{0.8}Ca_{0.2}CrO_3$	9.5	13.5	7.3
$La_{0.7}Ca_{0.3}CrO_3$	9.7	17.2	8.0
$La_{0.9}Sr_{0.1}CrO_3$	9.2	10.3	9.8
$La_{0.8}Sr_{0.2}CrO_3$	9.9	12.2	9.4
$La_{0.7}Sr_{0.3}CrO_3$	10.7	16.5	8.9

Table VI. All the perovskites showed a large difference between their TECs in air and the H_2 atmosphere during the second heating cycle. This leads to the generation of thermal stress in the SOFC separator at the operating condition [25]. In addition, it was observed that the TECs of the first heating cycle in the H_2 atmosphere were much larger than those during air and the second heating cycle in the H_2 atmosphere.

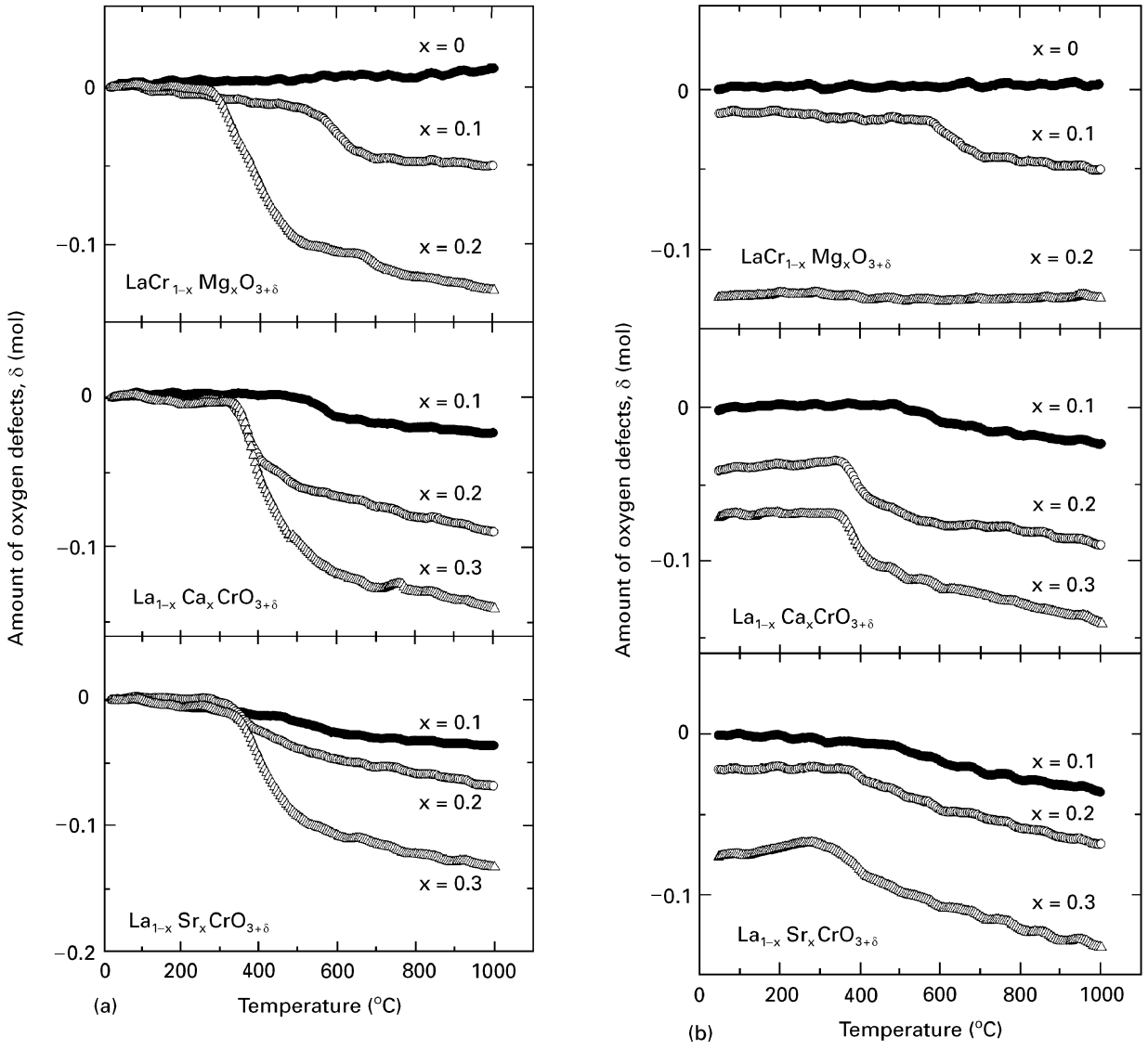

Figure 7 Amount of oxygen defects in the AE-doped lanthanum chromites as a function of temperature in the H_2 atmosphere: (a) first heating cycle; (b) second heating cycle.

Schafer and Schmidberger [4] have reported that the formation of oxygen defects in the Ca- or Sr-doped $LaCrO_3$ perovskites caused a large thermal expansion under the reducing atmosphere. Fig. 7a and b show the amount of oxygen defects in the AE-doped lanthanum chromites under the H_2 atmosphere as a function of temperature when the oxygen defects of the unfired perovskites are assumed to be zero at 25 °C in the H_2 atmosphere, for the first and second heating cycles, respectively [14]. A drastic weight decrease was observed for the AE-doped $LaCrO_3$; however, pure $LaCrO_3$ did not show this [26]. The weight loss, which corresponded to the oxygen defect formation by charge compensation of Cr^{4+} to Cr^{3+} ions, started at 333 °C for $La_{0.8}Ca_{0.2}CrO_3$ and at 315 °C for $La_{0.8}Sr_{0.2}CrO_3$ during the first heating cycle. In the second heating cycle, the oxygen defects of the AE-doped lanthanum chromites remained even at 50 °C, and the values at 1000 °C were equal to those of the first heating cycle. The temperatures of the oxygen defect formation were similar to those of the anomalies for the thermal expansion slopes or the phase transformations. It was clarified by using high-temperature XRD analysis that $La_{0.8}Ca_{0.2}CrO_3$ and $LaCr_{0.8}Mg_{0.2}O_3$ with the $GdFeO_3$-type perovskite structure underwent a phase transformation from rhombohedral to orthorhombic symmetry in the He (95%) –H_2(5%) atmosphere at approximately 300 °C. On the other hand, $La_{0.8}Sr_{0.2}CrO_3$ with $LaCoO_3$-type perovskite structure did not undergo a phase transformation although the angle of the Cr-O bond was closed to 90°. Therefore, we can conclude that the large thermal expansion behaviours of the AE-doped $LaCrO_3$ are related to the oxygen defect formation, and the high concentration of defects results in larger TECs. These results suggest that doped lanthanum chromites with a low AE content would be suitable as a separator in planar-type SOFCs.

4. Conclusions

The AE-doped lanthanum chromites have been examined for use as a separator in planar-type high-temperature solid oxide fuel cells. The thermal expansion of

doped $LaCrO_3$ separators in air are important because fabrication of the SOFC stack are usually in air by high-temperature heat treatments. On the other hand, separators placed in a SOFC stack are exposed to both an oxidizing and a reducing environment at the operating condition, and properties such as electrical conductivity and thermal expansion are essentially governed by those in the reducing atmosphere. The low electrical conductivity in the reducing condition is a serious problem because it limits the power density of the SOFC. Therefore, the AE dopant content should be as high as possible. However, AE doping should be limited because of the unexpected thermal expansions of the AE-doped lanthanum chromites from oxidizing to reducing atmosphere. Although the electrical conductivities of magnesium-doped lanthanum chromites were lower than those of the A-site substituted samples, $LaCr_{0.9}Mg_{0.1}O_3$ showed the highest mechanical strength, the highest thermal conductivity and the minimum mismatch between air and the reducing atmospheres. Furthermore, the observed volume change of $LaCr_{0.9}Mg_{0.1}O_3$ was not drastic from air to the reducing atmosphere. However, there still remains much research to match the TEC in air with yttria fully stabilized zirconia electrolyte.

References

1. B. F. FLANDERMEYER, M. M. NASRALLAH, D. M. SPARLIN and H. U. ANDERSON, *High Temp. Sci.* **20** (1985) 265.
2. W. J. WEBER, C. W. GRIFFIN and J.B. BATES, *J. Amer. Ceram. Soc.* **70** (1987) 265.
3. N. SAKAI, T. KAWADA, H. YOKOKAWA, M. DOKIYA and T. IWATA, *J. Mater. Sci.* **25** (1990) 4531.
4. W. SCHAFER and R. SCHMIDBERGER High Tech Ceramics edited by P. Vincenzini (Elsevier, Amsterdam, 1987) 1737.
5. J. MIZUSAKI, S. YAMAUCHI, K. FUEKI and A. ISHIKAWA, *Solid State Ionics* **12** (1984) 119.
6. S. SRILOMSAK, D. P. SCILLING and H. U. ANDERSON, in "Proceedings of the First International Symposium on Solid Oxide Fuel Cells" edited by S. C. Singhal, PV 89-11 (The Electrochemical Society, Pennington NJ, 1989) p. 129.
7. D. B. MEADOWCRAFT, *Brit. J Appl. Phys.* **2** (1969) 1225.
8. D. P. KARIM and A. T. ALDRED, *Phys. Rev. B* **20** (1979) 2255.
9. N. M. SAMMES, R. RATNARAJ and C. E. HATCHWELL, in "Proceedings of the Fourth International Symposium on Solid Oxide Fuel Cells" edited by S. C. Singhal and H. Iwahara, PV 93-4 (The Electrochemical Society, Pennington NJ, 1995) p. 952.
10. M. MORI, T. YAMAMOTO, H. ITOH and T. ABE, in " Proceedings of the Fourth International Symposium on Solid Oxide Fuel Cells" edited by M. Dokiya, O. Yamamoto, H. Tagawa and S. C. Singhal, PV 95-1 (The Electrochemical Society, Pennington NJ, 1995) p. 905.
11. M. MORI, N. SAKAI, T. KAWADA, H. YOKOKAWA and M. DOKIYA, *Denki Kagaku* **59** (1991) 314.
12. N. SAKAI, T. KAWADA, H. YOKOKAWA, M. DOKIYA and I. KOJIMA, *J. Amer. Ceram. Soc.* **76** (1993) 609.
13. J. MIZUSAKI, Y. MIMA, S. YAMAUCHI, K. FUEKI and H. TAGAWA, *J. Solid State Chem.* **80** (1989) 102.
14. J. MIZUSAKI, M. YOSHIHIRO, S. YAMAUCHI and K. FUEKI, *ibid.* **58** (1989) 257.
15. I. YASUDA and T. HIKITA, in " Proceedings of the Second International Symposium on Solid Oxide Fuel Cells" edited by F. Grosz, P. Zegers, S. C. Singhal and O. Yamamoto, Report EUR 13564 EN (Commission of European Communities, Luxembourg, 1991) p. 645.
16. I. YASUDA and T. HIKITA, "Proceedings of the Third International Symposium on Solid Oxide Fuel Cells" edited by S. C. Singhal and H. Iwahara, PV 93-4 (The Electrochemical Society, Pennington NJ, 1993) p. 345.
17. B. A. HASSEL, T. KAWADA, N. SAKAI, H. YOKOKAWA and M. DOKIYA, *Solid State Ionics* **66** (1993) 41.
18. T. KAWADA, T. HIROTA, N. SAKAI, H. YOKOKAWA and M. DOKIYA, in " Extended Abstracts of the 20th Commemorative International Symposium on Solid State Ionics in Japan" (Solid State Ionics Society Japan, Tokyo, 1994) p. 119.
19. K. OGASAWARA, I. YASUDA and M. HISHINUMA, in "Proceeding of the 61st Meeting of the Electrochemical Society Japan" 3–5 April (Electrochemical Society of Japan, 1994) p. 85.
20. Y. TAKEDA, R. KANNO, M. NODA and O. YAMAMOTO, *Bull. Inst. Chem. Res. Kyoto Univ.* **64** (1986) 157.
21. N. SAKAI, T. KAWADA, H. YOKOKAWA, M. DOKIYA and T. IWATA, in "Proceeding of the 57th Meeting of the Electrochemical Society of Japan" 5–7 April (Electrochemical Society of Japan, 1990) p. 270.
22. S. C. SINGHAL, S. K. LAW, R. J. RUKA and S. SINHAROY, Report DOE/MC/21184-T1 (1985).
23. N. SAKAI, T. KAWADA, H. YOKOKAWA, M. DOKIYA and T. IWATA, *Solid State Ionics* **40–41** (1990) 394.
24. N. SASAKI, S. OTOSHI, A . KAJIMURA, M. SUZUKI, H. OHNISHI, H. SASAKI and M. IPPOMMATSU, *J. Ceram. Soc. Japan.* **101** (1993) 769.
25. I. YASUDA and M. HISHINUMA, in "Proceedings of the Fourth International Symposium on Solid Oxide Fuel Cells" edited by M. Dokiya, O. Yamamoto, H. Tagawa and S. C. Singhal, PV 95-1 (The Electrochemical Society, Pennington NJ, 1995) p. 924.
26. T. NAKAMURA, G. PETZOW and L. J. GRAUCKLER, *Mater. Res. Bull.* **14** (1979) 649.

Received 30 November 1995
and accepted 19 December 1996